

# International Conference on Space Optics—ICSO 2012

Ajaccio, Corse

9–12 October 2012

*Edited by Bruno Cugny, Errico Armandillo, and Nikos Karafolas*



## *The optimization of the inverted occulter of the solar orbiter/METIS coronagraph/spectrometer*

*F. Landini*

*S. Vives*

*M. Romoli*

*C. Guillon*

*et al.*



# The optimization of the inverted occulter of the Solar Orbiter/METIS coronagraph/spectrometer

F. Landini<sup>1</sup>, S. Vives<sup>2</sup>, M. Romoli<sup>1</sup>, C. Guillon<sup>2</sup>, M. Pancrazzi<sup>1,2</sup>, C. Escolle<sup>2</sup>, M. Focardi<sup>1</sup>, S. Fineschi<sup>3</sup>, E. Antonucci<sup>3</sup>, G. Nicolini<sup>3</sup>, G. Naletto<sup>4</sup>, P. Nicolosi<sup>4</sup>, D. Spadaro<sup>5</sup>

<sup>1</sup>Department of Physics and Astronomy – Section of Astronomy, University of Firenze, Firenze, Italy

FL: [flandini@arcetri.astro.it](mailto:flandini@arcetri.astro.it); MR: [romoli@arcetri.astro.it](mailto:romoli@arcetri.astro.it); MP: [panc@arcetri.astro.it](mailto:panc@arcetri.astro.it); MF: [mauro@arcetri.astro.it](mailto:mauro@arcetri.astro.it)

<sup>2</sup>Aix Marseille Université, CNRS, LAM (Laboratoire d'Astrophysique de Marseille) UMR 7326, 13388, Marseille, France  
SV: [sebastien.vives@oamp.fr](mailto:sebastien.vives@oamp.fr); CG: [christophe.guillon@oamp.fr](mailto:christophe.guillon@oamp.fr); CE: [clement.escolle@oamp.fr](mailto:clement.escolle@oamp.fr)

<sup>3</sup>INAF – Osservatorio Astrofisico di Torino, Pino Torinese, Torino, Italy  
SF: [fineschi@oato.inaf.it](mailto:fineschi@oato.inaf.it); EA: [antonucci@oato.inaf.it](mailto:antonucci@oato.inaf.it); GN: [nicolini@oato.inaf.it](mailto:nicolini@oato.inaf.it)

<sup>4</sup>Department of Information Engineering, University of Padova, Padova, Italy

GN: [naletto@dei.unipd.it](mailto:naletto@dei.unipd.it); PN: [nicolosi@dei.unipd.it](mailto:nicolosi@dei.unipd.it)

<sup>5</sup>INAF – Osservatorio Astrofisico di Catania, Catania, Italy

DS: [spadaro@oact.inaf.it](mailto:spadaro@oact.inaf.it)

**Abstract**—The coronagraph/spectrometer METIS (Multi Element Telescope for Imaging and Spectroscopy), selected to fly aboard the Solar Orbiter ESA/NASA mission, is conceived to perform imaging (in visible, UV and EUV) and spectroscopy (in EUV) of the solar corona. It is an integrated instrument suite located on a single optical bench and sharing a unique aperture on the satellite heat shield. As every coronagraph, METIS is highly demanding in terms of stray light suppression. In order to meet the strict thermal requirements of Solar Orbiter, METIS optical design has been optimized by moving the entrance pupil at the level of the external occulter on the S/C thermal shield, thus reducing the size of the external aperture. The scheme is based on an inverted external-occulter (IEO). The IEO consists of a circular aperture on the Solar Orbiter thermal shield. A spherical mirror rejects back the disk-light through the IEO. The experience built on all the previous space coronagraphs forces designers to dedicate a particular attention to the occulter optimization. Two breadboards were manufactured to perform occulter optimization measurements: BOA (Breadboard of the Occulting Assembly) and ANACONDA (AN Alternative Configuration for the Occulting Native Design Assembly). A preliminary measurement campaign has been carried on at the Laboratoire d'Astrophysique de Marseille. In this paper we describe BOA and ANACONDA designs, the laboratory set-up and the preliminary results.

**Keywords:** Solar coronagraph, external occulter, optimization, stray light, measurements, Solar Orbiter, METIS

## I. INTRODUCTION

The Solar Orbiter ESA/NASA mission [1], currently in phase C, will approach the Sun by reaching a perihelion of 0.28 astronomical units (AU) and orbiting up to 30° out of the ecliptic. It constitutes the next major step forward in the exploration of the Sun and the heliosphere after the successful missions of the last 20 years. The Multi-Element Telescope for Imaging and Spectroscopy (METIS) [2], selected to fly aboard the Solar Orbiter, is a coronagraph/spectrometer designed to

perform imaging and spectroscopy of the solar corona by means of an integrated instrument suite located on a single optical bench and sharing a unique aperture on the satellite heat shield. In particular METIS will provide for the first time:

- simultaneous imaging of the full corona in polarized visible-light (590-650 nm) and narrow-band ultraviolet HI Ly  $\alpha$  (121.6 nm);
- monochromatic imaging of the full corona in the extreme ultraviolet HeII Ly  $\alpha$  (30.4 nm);
- spectroscopic observations of HeII Ly  $\alpha$  in corona.

These measurements will allow a complete characterization of the three most important plasma components of the corona and the solar wind (electrons, protons, helium).

In order to match the strict mission requirements in terms of mass and heat control, a creative effort was performed in order to squeeze the three METIS channel on a single optical bench and to take advantage of a single aperture on the spacecraft (S/C) thermal shield. An innovative occulter principle was developed in order to deal with the mission challenges. A deeper insight into the instrument optical design is presented in section II. Like every coronagraph, METIS requires highly effective stray light suppression. Past experiences on space coronagraphy teach us that the occulter edges are the major source of stray light and that in the design process particular attention must be dedicated to optimizing the occulter. The light diffracted by the occulter edge and scattered by the telescope optics constitutes a contribution of the same order of magnitude of the coronal light. It has been demonstrated by all the previous successful coronagraphic missions that an occulter edge shape optimization may lower the level of diffracted light by 2 or 3 orders of magnitude.

However in the case of METIS, it is not possible to reproduce previous configurations. Indeed to cope with the

extreme thermal load (~10 times the one at 1AU), an innovative occulting system, allowing to drastically reduce the aperture in the thermal shield (by about a factor 2) has been proposed.

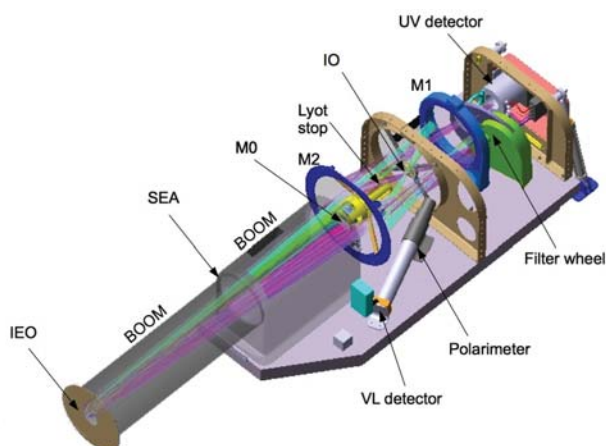
In this paper we describe the concept we adopted to pursue the optimization of the innovative METIS occulter (section III), the two METIS occulting system prototypes we designed and the laboratory set-up we assembled (sections IV and V); finally we describe some preliminary results that we obtained during the preliminary test campaign at the LAM (Laboratoire d'Astrophysique de Marseille, France) solar simulator (section VI).

## II. OPTICAL DESIGN

Fig. 1 shows a 3D sketch of the METIS coronagraph, with emphasis on the main optical elements described in this section. METIS is designed around an innovative concept for externally occulted solar coronagraph, based on an inverted external-occulter (IEO) [3, 4]. The IEO is a small circular aperture which replaces the classical annular aperture of the standard externally occulted solar coronagraph design. A boom connects the IEO to the M0, a small spherical mirror that rejects back the disk-light through the IEO. Many are the advantages of this novel design with respect to the classical one. Considering its application to this instrument, they can be summarized in the following points:

- smaller external occulter diameter;
- thermal load on M0 greatly reduced;
- on-axis telescope configuration;
- more compact, cylindrical structure.

The smaller external occulter diameter implies a smaller aperture on the S/C thermal shield; the reduced thermal load produces a lower temperature inside the instrument and a better stability and control of the optical bench; the on-axis configuration gives better optical performance, and has the advantage of a simpler mechanical structure; the compactness of the structure allows to optimize the available resources, and the cylindrical structure gives a symmetric configuration and an easier baffling, which is always an extremely critical point for solar coronagraphy. Beyond M0, an on-axis annular shape Gregorian telescope focuses the solar corona on the focal plane assembly. The Gregorian configuration of the primary and the secondary mirror, respectively M1 and M2, gives access to the primary focal plane for the placement of the internal occulter (IO). The IO blocks the light diffracted by the edge of the IEO and reflected by M1.



A Lyot stop positioned slightly after the IO blocks the light diffracted by M0 and reflected by M1. A filter wheel positioned just in front of the UV detector allows to select either visible and/or UV/EUV (HI 121.6 nm or HeII 30.4 nm line) images of the corona. When the thin aluminum filter is in the path, only HeII observations are performed. When the Al/MgF<sub>2</sub> interference filter is in the path, the HI light is transmitted to the UV detector, while the broadband visible light (VL) is reflected towards the liquid crystal polarimeter, in order to perform measurements of the linear polarization of the visible solar corona.

To improve the scientific return of this instrument, a spectroscopic channel has also been included in the METIS optical path. Essentially, in the prime focus of the Cassegrain telescope, a three slit system is located in correspondence of an equatorial region of the solar corona; this slit system inhibits the possibility of doing imaging in this portion of the corona, so the actual coronal images of METIS will have a small sector missing. Light passing through the slits is collected by a diffraction grating located in a sector of the Cassegrain telescope secondary mirror. UV light is then dispersed and focused on the same UV/EUV detector used for imaging.

## III. THE METIS OCCULTER OPTIMIZATION CONCEPT

Since the very first experiment on occulter optimization by Newkirk and Bohlin in 1965 [5], the quest of the best optimizing shape has triggered the efforts of generations of solar coronagraphs designers. From literature [5-10] we selected the polished cone as optimizing shape, because it is relatively easy to manufacture while granting a high efficiency in reducing the stray light.

The unconventional occulting principle of METIS leads us to adapt the truncated cone optimizing principle to an inverted truncated cone. Fig. 2 shows a comparison between the cone (top) and the inverted cone (bottom) configurations. In order to simplify the description, only sections of the whole geometry are represented. The external inverted cone surface is shaped following the geometry of the internal surface in order to expose the minimum amount of occulter surface to the M0 back scattered light.

The two main geometrical parameters that define an inverted cone are the cone angle and the cone length (see Fig. 2).

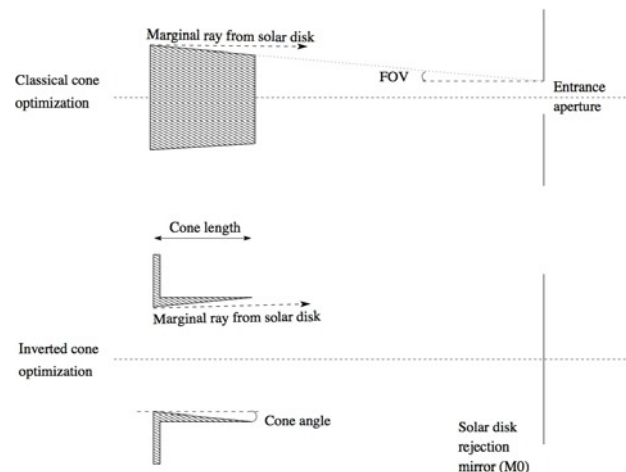


Figure 2. Section sketch showing a comparison between the cone (top) and the inverted cone (bottom) optimizations.

The occulting system optimization is performed either by adjusting the shape of the occulter and by defining the geometry and the manufacturing parameters of the boom.

The boom is equipped with a series of vanes that prevent light scattered first by the IEO edge and then once by the boom internal surface to impinge on the M1 plane. In fact, the stray light arriving on the M1 surface would be scattered by M1 and thus follow the same path of the coronal light, while the stray light passing through the M1 aperture would directly impinge onto the focal planes.

The boom is a critical element in interfacing METIS with the Solar Orbiter S/C. The front part of the boom (from the IEO to the Shield Entrance Aperture, SEA, diaphragm, see Fig.1) is designed to be inserted in the S/C thermal shield, thus it requires careful mechanical and thermal optimization, besides the internal stray light suppression configuration.

Being the boom the most critical interface, thus subject to likely structural modifications throughout the missions phases, we decided to manufacture two prototypes in order to span the widest possible range of geometries: BOA (Breadboard of the Occulting Assembly) and ANACONDA (AN Alternative Configuration for the Occulting Native Design Assembly), that are thoroughly described in the next section.

#### IV. THE TWO PROTOTYPES

BOA and ANACONDA are cylindrical assemblies with the IEO on one side and a detector on the other side, positioned on the M1 plane.

In order to evaluate the contribution given by the vanes and by the boom geometry, both prototypes share some manufacturing characteristics:

- vanes can be easily implemented and removed;
- the front part includes a sliding adjusted hole H7/g6 that allows the implementation of different occulters without losing the tube alignment with the source;
- the back part is equipped with a motorized translation stage carrying a calibrated photodiode (CPD) that scans one diameter of M1 (the stray light pattern on M1 has circular symmetry);
- the mechanics that is used to hold and align M0 is the same in both prototypes.

Fig. 3 shows the most evident geometric difference between BOA and ANACONDA, that is the diameter of the section of the boom that must be inserted in the S/C thermal shield. ANACONDA is characterized by a constant diameter. BOA is designed accordingly to the original METIS design that foresees two boom sections with different diameters, the smaller one to be inserted in the S/C thermal shield.

The difference between the two prototypes allows evaluating the impact of the boom geometry on the stray light reduction performance.

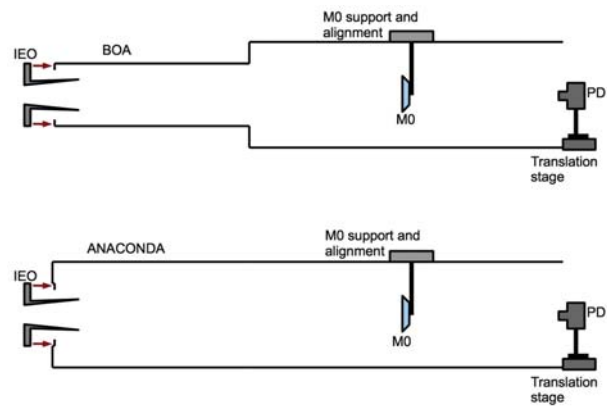


Figure 3. Sketch showing the basic geometric difference between BOA (top) and ANACONDA (bottom).

Fig. 4 shows a picture of the two prototypes positioned close to each other.

By comparison with BOA, ANACONDA is crucial in identifying the various contributors to the total stray light level on the focal plane. The measurements described in Table I, allow investigating the role of each stray light source.

The Vel Black<sup>®</sup> cited in the table is an absorbing coating characterized by a very low reflectance (< 0.5 %) over a broad wavelength band (UV-VIS-mid IR). It is used in order to separate the contribution given by the back scattering of the M0 mirror from the other stray light sources.

We planned the measurement activity according to the strategy summarized by the following list.

- 1) Find the best trade off geometry (cone length and angle, see Fig. 2) with the coronagraph at its perihelion (0.28 AU);
- 2) evaluate the performance of the optimization found at step (1) at different distances from the Sun. If the performance worsen to an unacceptable level (i.e., comparable to the not-optimized occulter), then another solution must be found at step (1).
- 3) Evaluate the performance of the occulter optimized after steps (1) and (2) in case of coronagraph off-pointing.

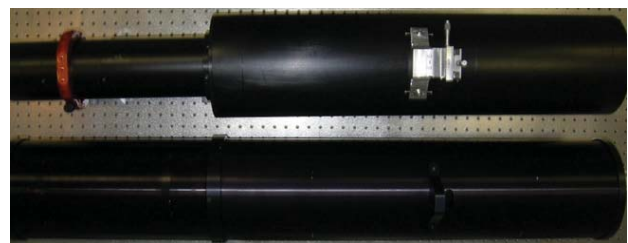


Figure 4. Picture of BOA and ANACONDA positioned close to each other on an optical bench.

TABLE I. SET OF MEASUREMENTS TO BE PERFORMED WITH BOA AND ANACONDA TO IDENTIFY THE VARIOUS STRAY LIGHT SOURCES

Prototype	M0	Occluder	Vanes	Usefulness
Both	VB <sup>a</sup>	Simple aperture	Full set	Evaluate the impact of the boom geometry (section VI.D)
Both	Mirror	Simple aperture	Full set	Evaluate the combined effect M0 mirror/boom geometry
One of the two	VB <sup>a</sup>	Simple aperture	Without/With	Evaluate the impact of the vanes (section VI.C)
One of the two	Mirror	Simple aperture	Without/With	Evaluate the combined effect M0 mirror/Vanes inner edge
One of the two	VB <sup>a</sup>	Cones: fixed length, all angles	Full set	Select the best cone angle (section VI.A)
One of the two	VB <sup>a</sup>	Cones: fixed angle, all lengths	Full set	Select the best cone length (section VI.B)
One of the two	VB <sup>a</sup>	Simple aperture, flat/sharp edge	Full set	Evaluate the impact of the edge shape and of its coating (section VI.E)
One of the two	Mirror	Simple aperture, flat/sharp edge	Full set	Evaluate the combined effect of the edge shape/coating and the M0 mirror
One of the two	Mirror	Cone: the best solution	Full set	Evaluate the impact of M0 mirror in the optimized case
One of the two	VB <sup>a</sup>	One of the cones, with various tilts	Full set	Evaluate the impact of a bad IEO alignment during the integration (section VI.F)
One of the two	Mirror	One of the cones, with various tilts	Full set	Evaluate the combined effect of M0 and a bad IEO alignment during the integration.
One of the two	Mirror	Shiny occulter	Full set	Evaluate the back scattering of the IEO internal surface in combination with the M0 reflection.

a. VB: Vel Black<sup>®</sup> (by Energy Science Laboratory, Inc.)

As shown in Fig. 2, the cone angle must be larger than the angle subtended by the solar disk, otherwise the bright solar disk light will graze the inner surface of the inverted cone and become a major stray light source. Due to the mission characteristics, the angle subtended by the disk is going to change continuously. An upper limit to such dimension is given by the angle subtended by the solar disk when the Solar Orbiter is at its perihelion. With the spacecraft at the perihelion, the angle subtended by a solar radius is  $\sim 0.955^\circ$ . A cone angle of  $1.000^\circ$  gives a minimum over-occultation of  $1.05 R_\odot$  ( $1 R_\odot \sim 7 \times 10^{10}$  cm is the solar radius). We manufactured cones with different angle in order to evaluate the impact of the cone angle to the stray light suppression performance. Several cone lengths were applied as well. Table II classifies all the manufactured cones in terms of cone angle and length. An overall view of the occulter is shown in Fig. 5.



Figure 5. Picture of all the manufactured occulter.

The inverted cones have been manufactured in black anodized Aluminum by means of a numerical control lathe, that guarantees an uncertainty within  $\sim 5$  arcsec on the cone angle. A simple knife edge aperture was considered as a reference for all the tests, and all the results have been normalized to the unobstructed source integrated flux. We also left one of the knife edge apertures uncoated, in order to get a first order evaluation of the impact that the coating may yield. Following the results obtained in a previous work [10], we decided that as a first step of our investigation we may neglect the impact given by the material on the optimization performance.

## V. THE EXPERIMENTAL SET-UP

The two prototypes share the same kind of interface with an optical rail that works as support and alignment tool. The source is a solar simulator (i.e. a laboratory facility which simulates the angular dimension of the Sun as seen from a certain distance).

TABLE II. CLASSIFICATION OF THE MANUFACTURED CONES

IEO LIST		Cone angles (deg)				
		1.076	1.000	0.604	0.302	0.280
Cone lengths (mm)	30	×	×	×	×	×
	70	×	×	×	×	
	100	×	×			

As described in section IV, the tests have to be performed in front of a solar simulator characterized by a modifiable dimension, to simulate the different positions of the Solar Orbiter S/C respect to the real Sun.

In order to frame the main challenging issues in performing the tests, to find practical solutions and to get a first set of results on cone and boom performance, a preliminary tests campaign was run at the Laboratoire d'Astrophysique de Marseille (LAM), in France. The LAM solar simulator is characterized by a fixed diameter of  $\sim 32$  arcmin that corresponds to an observer's distance of 1 AU from the Sun. A satisfactory description of the solar simulator facility can be found in [9].

The preliminary measurement campaign at LAM was characterized by some peculiarities:

- Only Vel Black<sup>®</sup> coated M0 was used.
- The solar simulator has a fixed size of 32 arcmin.
- M0 was resized in order to match, with the LAM Sun dimension, the same nominal field of view of METIS at its perihelion

Fig. 6 shows BOA installed in front of the LAM solar simulator in a class 100 (ISO 5) clean room, that has been the environment for the whole measurements campaign.

A final test campaign will be run at the new OPSys [11] facility in Torino (Italy) that hosts a solar simulator with modifiable dimensions assembled in a vacuum tank. The first part of the final campaign will be a replica of the LAM campaign, in order to validate the OPSys facility and to evaluate possible performance differences between the two solar simulators. The second part of the final campaign will be used to define and freeze all the geometrical and manufacturing characteristics of the optimized occulter for the METIS coronagraph.

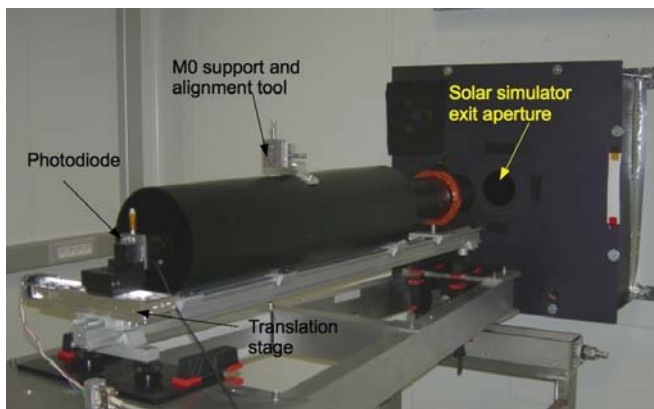


Figure 6. Picture of BOA in front of the LAM solar simulator.

## VI. PRELIMINARY RESULTS

A first test was performed with the CPD in front of the solar simulator exit aperture, in order to evaluate the uniformity of the source. The Sun is uniform within the 95% over a diameter of 40 mm centered on the Sun axis, that is the dimension of the IEO aperture.

In the following sub-sections we describe the comparative analysis we performed with the different occulter and the two prototypes.

### A. Cone angle and two-peaks behaviour

Fig. 7 shows the comparison between five different inverted cone angles for a fixed length of 30 mm.

While noticing that the inverted cone optimization indeed reduces the stray light level on the M1 plane respect to the simple circular aperture configuration, we point out the different behaviour of the two kinds of curve. The curve relative to the simple circular aperture shows a peak of diffraction in correspondence of the M0 edge projection on the

M1 plane: the level of the peak is in the  $10^{-4}$  range, since the edge of M0 is in the shadow of the IEO edge respect to the solar disk light, thus M0 diffracts the light diffracted by IEO.

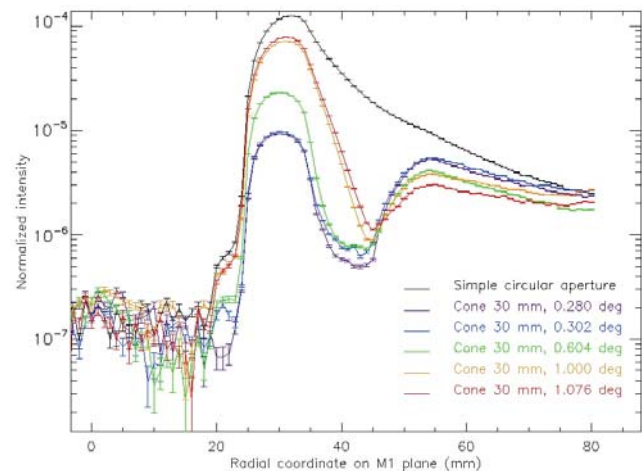


Figure 7. Comparison of five different inverted cone angles for a fixed length of 30 mm. The simple knife edge aperture is taken as a reference.

The curves relative to the inverted cones are characterized by two peaks, which origin is explained in Fig. 8.

Moving with the CPD from the point on-axis towards the M1 edge, there is a first peak, given by the diffraction from the M0 edge of the light diffracted by the inverted cone. It is the same peak that is present in the simple circular aperture curve.

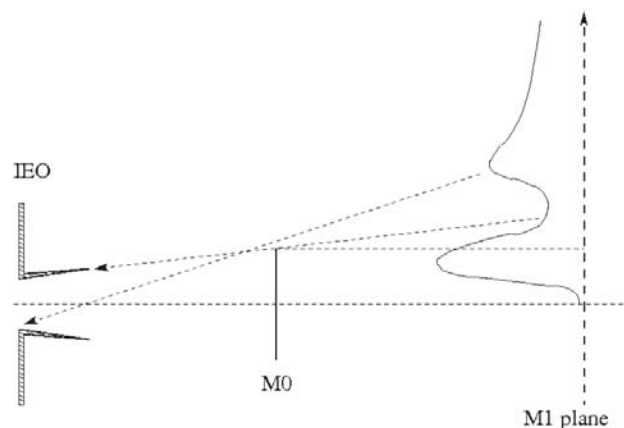


Figure 8. Scheme that justifies the two-peaks behaviour of the inverted cone stray light curves on the M1 plane.

Then there is a decrease, that corresponds to the vignetting action of the external surface of the inverted cone, that occults the IEO aperture as seen from the M1 plane. The minimum of the descent does not correspond to an absence of signal because there still is a contribution given by the light scattered first by the cone outer edge and then either directly by the boom surface, or before from the cone surface and after from the boom internal surface (see also section VI.D). Still moving towards the edge of M1, while the vignetting action of the cone

terminates, the stray light on the M1 plane increases to match the nominal stray light pattern of the simple circular aperture. The junction of the two effects (the nominal diffraction curve and the ending action of the cone) gives rise to the second peak. A small contribution to the second peak is also given by scattering by the internal surface of the cone of the light diffracted by the edge: this generates higher levels of stray light as the cone angle is reduced. In fact, from Fig. 7 it is easy to notice that the second peak levels are sorted in inverted order respect to the first peak levels. After the second peak, the curve slowly approaches the nominal behaviour of the simple aperture stray light.

Fig. 7 also shows that the cone angle has a huge impact on the stray light suppression performance. The inverted cone angle optimized for the LAM Sun configuration, i.e.  $0.280^\circ$ , greatly reduces the amount of stray light on the M1 plane respect to the simple aperture. The  $1.076^\circ$  and  $1^\circ$  cones have a much worse effect, since the vignetting action of the cone surface is almost completely wasted by the large angular aperture.

### B. Cone length

Fig. 9 compares three different cone lengths for a fixed cone angle of  $1.000^\circ$ . It is evident that, at least up to a cone length of 100 mm, the length has no significant impact on the stray light suppression performance of the inverted cone.

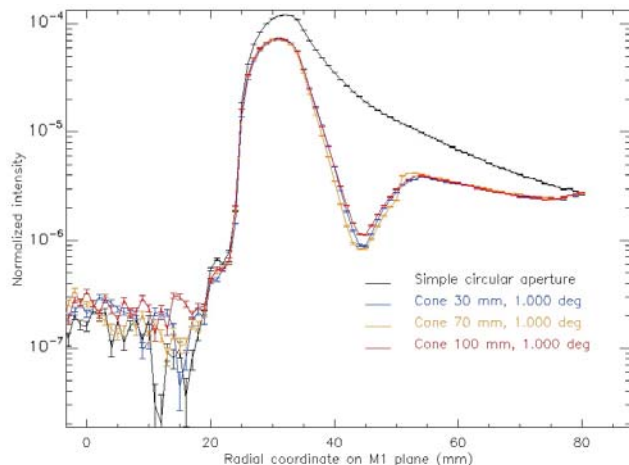


Figure 9. Comparison of three different cone lengths for a fixed cone angle of  $1.000^\circ$ . The simple knife edge aperture is taken as a reference.

### C. Vanes

Fig. 10 shows the performance evaluation in three different vanes configurations:

- without any vanes installed;
- with only the vane that simulates the vignetting action of M2;
- with the complete set of vanes.

In the case of Fig. 10, the tests were performed with BOA and a simple circular aperture as occulter, with the Vel Black coated M0 in place.

Without vanes, a huge amount of light diffracted from the IEO edge is scattered by the boom internal surface towards the M1 plane. A major fraction of this light enters the M1 aperture, directly impinging on the filter wheel and thus on the detectors; a smaller contribution is also given to the curve tail towards the edge of M1.

The M2 simulator is a diaphragm that acts as a vane, blocking a portion of the light that is scattered by the boom surface. Both the central and the side contributions to the stray light on the M1 plane are greatly reduced.

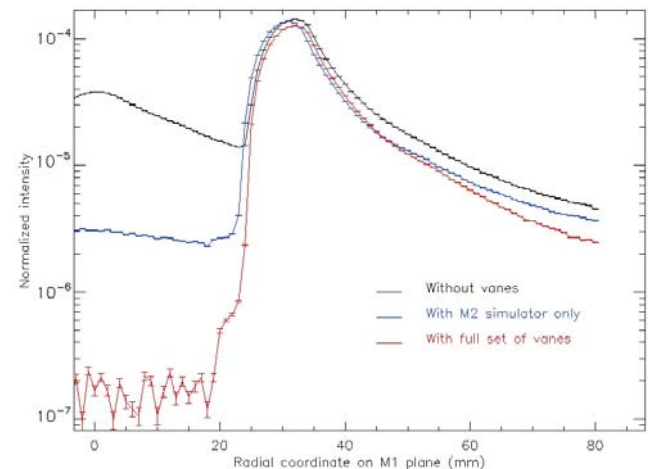


Figure 10. Impact of the vanes on the stray light reduction performance.

The measurement with the full set of vanes demonstrate the usefulness of the vanes: the stray light in the central part of M1 is reduced by about two orders of magnitude and even the level at the edge of M1 is less than a half respect to the case without vanes.

Measurements of the same kind with ANACONDA give the same relative performance in the three cases, thus no additional plot needs to be shown.

### D. Boom geometry

Fig. 11 shows the comparison between the performance of BOA and ANACONDA in terms of stray light reduction. The comparison is shown only for a cone 30 mm long and with an angle of  $0.302^\circ$ , but the relative behaviour is the same for all the cones.

The differences between the performance of BOA and ANACONDA are rather small, but they cannot be neglected. The most significant difference is in the part of the stray light curve between the first peak and the valley. While the two peaks are almost overlapped (difference  $\sim 14\%$ ), the two valleys are quite separated (difference  $\sim 52\%$ ).

The measurements were performed with the optimal vanes configuration for both prototypes. The difference in the

behaviour is due to multiple scattering by the boom surface of the light diffracted by IEO. The smaller diameter of the BOA front part of the boom favours a higher number of scattering interactions between stray light and the boom surface.

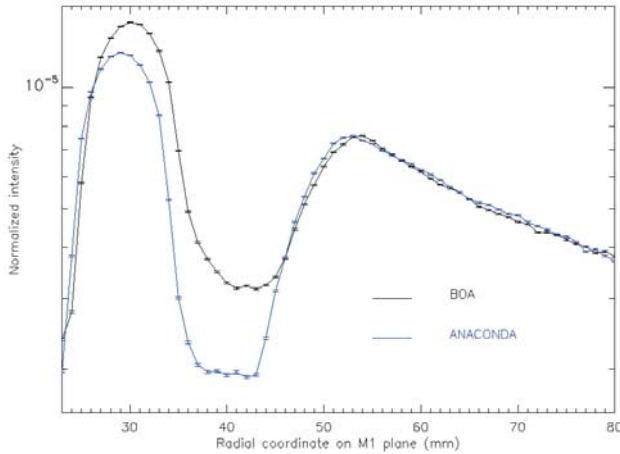


Figure 11. Comparison between BOA and ANACONDA performance by using the same inverted cone (length 30 mm, angle 0.302°).

### E. Occulter edge

Two different versions were manufactured of the simple aperture IEO, in order to evaluate the impact of the edge mechanical finishing on the stray light performance: a sharp edge and a flat edge version.

Fig. 12 shows the geometrical manufacturing difference between the two edge types.

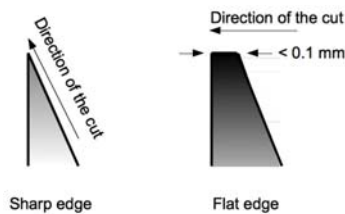


Figure 12. Geometrical manufacturing difference between the two edges of the simple circular aperture.

Both occulter are made of Aluminum.

The sharp edge is first hewed-out according to the geometrical shape of the occulter, then it is black anodized and finally cut along the chamfer of the edge without any further touch: the resulting knife edge is shiny and may present digs.

The flat edge occulter is accurately manufactured before the anodization, and a specific shape has been specified for the edge, cut along the occulter symmetry axis with a required edge thickness below 0.1 mm.

The two occulter generate the same stray light pattern on the M1 plane. The same kind of test will have to be replicated with a real mirror in place of Vel Black® on M0 (see Table I): a

shiny edge may prove a worse solution, since it may scatter towards the M1 plane the light back-scattered by M0.

A much more detailed work on the impact that the edge finishing and coating may have on stray light performance is described in [12].

### F. Occulter tilt

Some tilts were applied while attaching the occulter to the front part of the prototypes, in order to simulate an inaccurate alignment during the integration procedure.

The tilts were achieved by inserting calibrated spacers from 0  $\mu\text{m}$  up to 100  $\mu\text{m}$  between the occulter and the prototype front face, on one side of the prototype centering shape (i.e., in correspondence of the side of the prototype that was facing the east limb of the solar simulator). We achieved tilts ranging from 0 arcmin to 6 arcmin.

The stray light pattern on the M1 plane has circular symmetry, if no tilt is applied. Due to the prototype design, the impact of a tilt applied along the East-West direction (within a solar simulator centered frame of reference) should be detected along the direction of translation of the CDP on the M1 plane. By identifying a Cartesian coordinate system on M1, with the x axis coincident with the radial direction that has been used in all the shown plots and the z axis along the optical axis (from the IEO towards the M1), we define  $Y_r$  as the normalized stray light corresponding to the positive direction of the x axis and  $Y_l$  as the stray light corresponding to the negative direction of the x axis.

Fig. 13 shows the ratio between  $Y_r/Y_l$  obtained with a certain tilt and the  $Y_r/Y_l$  in the nominal configuration (i.e., with no tilt).

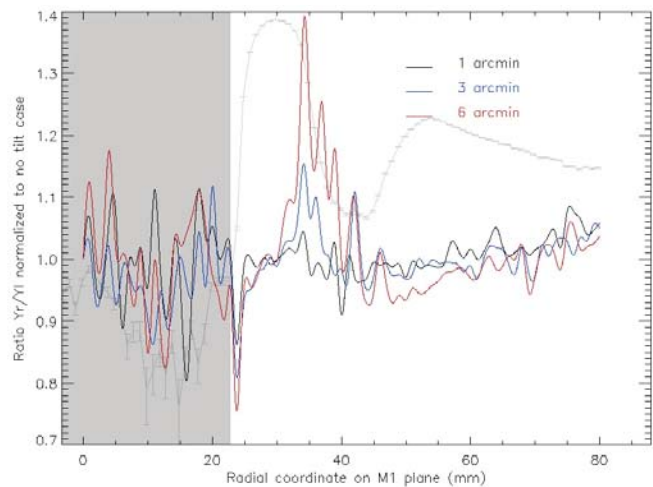


Figure 13. Evaluation of the tilt applied to the IEO integration. The plot is overlapped to a typical stray light pattern shape (without a reference scale) generated by an inverted cone.

The part shadowed in grey is not significant, since the detected signal is mainly due to the noise of the CPD. The

whole plot is overlapped to a typical stray light pattern as generated by an inverted cone (without a reference scale), in order to identify at a glance which part of the stray light pattern on M1 shows the most significant deviations from the nominal behaviour (i.e., identically 1).

The greatest impact of the applied tilt is on the descent from the first peak, that is given by light scattered first from the cone outer edge, then either from the cone or the boom internal surfaces (see Fig. 8 and the explanation in the text in section VI.A). The bad alignment of the IEO produces a greater amount of scattered light that the vanes are not able to block, and consequently a higher level of stray light on the M1 plane.

A tilt of the surface of IEO that is facing M0 may have a much bigger impact to the stray light when a real mirror is installed in place of Vel Black: this test will have to be replicated during the official measurements at OPSys (see Table I and section V).

### G. Occulter coating

Two types of sharp occulter were manufactured (see Fig. 12): one was black coated before the cut, the other was left uncoated. The comparison of the performance of the two occulters may give information on the impact of the IEO coating on the stray light pattern on M1.

The performed tests showed no appreciable differences. This leads to conclude that a black coating of the occulter may influence the stray light reduction performance only when a real mirror is installed on M0. The same test will have to be replicated during the measurements campaign at OPSys (see Table I).

## VII. CONCLUSION

A preliminary test campaign was run at the Laboratoire d'Astrophysique de Marseille in order to initiate the inverted external occulter optimization for the METIS coronagraph, selected to fly aboard the Solar Orbiter mission.

An inverted cone geometry is the optimization technique we chose to adopt for the METIS occulter. Two breadboards of the occulting assembly, BOA and ANACONDA, were manufactured in order to find the best cone geometry trade-off while coping with possible variations in the coronagraph boom design.

BOA and ANACONDA simulate the coronagraph section from the occulter to the primary objective plane and were used to evaluate the stray light pattern generated by different occulters on the primary mirror plane itself. By means of the prototypes, the cones can be compared while keeping a fixed mechanical supporting reference.

The tests were fundamental to frame the main challenges we have to deal with and to fix most of the problems. Moreover, the tests gave also some important results on the impact that the cone and the boom geometries have on the stray light suppression performance.

The cone angle is a key parameter in determining the performance, while from these preliminary tests it seems that no big influence is given by the cone length.

The boom diameter must be designed as large as the S/C thermal shield constraints may allow, since we demonstrated that the smaller the diameter, the higher the stray light contribution impinging on the primary mirror plane. Moreover, a full set of vanes is necessary inside the boom: without, a stray light level worsening of more than 2 orders of magnitude may be expected on the M1 plane.

We performed also some additional tests by comparing different simple circular aperture occulter coatings (shiny and black) and edges (sharp and flat): no impact has been detected onto the stray light pattern.

We applied calibrated tilts at the occulter integration, to detect whether and how a tilt can modify the occulting system performance. A disturbance proportional to the applied tilt is given to the light scattered by the cone and the boom surfaces.

All the tests were performed with a fixed solar disk dimension and with an absorbing coating on the solar disk light rejection mirror, M0. The use of a real mirror instead on M0 is likely going to change some of the results and is foreseen as part of the final measurement campaign.

The final measurement campaign will be carried on at the OPSys facility in Torino, a solar simulator with a dynamically modifiable configuration, able to simulate different solar disk dimensions, such as those that the Solar Orbiter will have to face during the mission.

### ACKNOWLEDGMENT

The authors are grateful to Jose Garcia for his willingness and all his fundamental suggestions. A special thanks must be reserved to Gilles Arthaud that was able to solve many technical and mechanical problems despite the short available time. Enzo Turchi has been a key person in the fine hand manufacturing of important mechanical pieces: to him we reserve most of our gratitude. Finally, thanks to Nataly Garcia Manzone, without whom the measurement campaign would not have even logistically started.

The LAM team was funded by CNES in the framework of the french participation to the Solar Orbiter mission.

The Italian team thanks the Italian Space Agency (contract number I/043/10/0) for technical, management and financial support.

### REFERENCES

- [1] ESA. Solar Orbiter Assessment Study Report, Tech. Rep. SRE(2009)5, 2009.
- [2] E. Antonucci et al., "Multi element telescope for imaging and spectroscopy (METIS) coronagraph for the Solar Orbiter", Proc. SPIE, vol. 8443, 2012, in press.
- [3] Fineschi, S., "Inverted-COR: Inverted-Occultation Coronagraph for Solar Orbiter," Tech. Rep. 119, INAF - Osservatorio Astronomico di

- Torino,  
[http://www.oato.inaf.it/biblioteca/pdf/TechRep119\\_Fineschi.pdf](http://www.oato.inaf.it/biblioteca/pdf/TechRep119_Fineschi.pdf), 2009.
- [4] S. Fineschi et al., "METIS: a novel coronagraph design for the Solar Orbiter Mission", Proc. SPIE, vol. 8443, 2012, in press.
- [5] G. Newkirk, Jr. and D. Bohlin, "Reduction of scattered light in the coronagraph", App. Opt., vol. 2(2), pp. 131-140, 1963.
- [6] B. Fort, C. Morel and G. Spaak, "The reduction of scattered light in an external occulting disk coronagraph", A&A, vol. 63, pp. 243-246, 1978.
- [7] A. V. Lenskii, "Theoretical evaluation of the efficiency of external occulting systems for coronagraphs", Sov. Astron., vol. 25(3), pp. 366-372, 1981.
- [8] S. Koutchmy, "Space born coronagraphy", Sp. Sc. Rev., vol. 47, pp. 95-143, 1988.
- [9] M. Bout, P. Lamy, A. Maucherat, C. Colin and A. Llebaria, "Experimental study of external occulters for the Large Angle and Spectrometric Coronagraph 2: LASCO-C2", App. Opt., vol. 39(22), pp. 3955-3962, 2000.
- [10] F. Landini, S. Vives, M. Venet, M. Romoli, C. Guillon and S. Fineschi, "External occulter laboratory demonstrator for the forthcoming formation flying coronagraphs", App. Opt., vol. 50(36), pp. 6632-6644, 2011.
- [11] S. Fineschi et al., "OPSys: optical payload systems facility for testing space coronagraphs", Proc. SPIE, vol. 8148, pp. 81480W-81480W-10, 2011.
- [12] S. Vives, C. Guillon, M. Pancrazzi, C. Escolle, J. Garcia, F. Landini, "Optimization of edge shape for stray light reduction", Proc. ICSO, 2012.